Femtosecond ultraviolet-visible absorption study of all - trans 13- cis 9- cis photoisomerization of retinal

Shoichi Yamaguchi and Hiro-o Hamaguchi

Citation: The Journal of Chemical Physics **109**, 1397 (1998); doi: 10.1063/1.476692
View online: http://dx.doi.org/10.1063/1.476692
View Table of Contents: http://scitation.aip.org/content/aip/journal/jcp/109/4?ver=pdfcov
Published by the AIP Publishing

Femtosecond ultraviolet-visible absorption study of all-*trans*→13-*cis*·9-*cis* photoisomerization of retinal

Shoichi Yamaguchi[a)]
Department of Basic Science, Graduate School of Arts and Sciences, The University of Tokyo, 3-8-1 Komaba, Meguro, Tokyo 153, Japan

Hiro-o Hamaguchi[b)]
Department of Chemistry, School of Science, The University of Tokyo, 7-3-1 Hongo, Bunkyo, Tokyo 113, Japan

(Received 31 December 1997; accepted 14 April 1998)

The all-*trans*→13-*cis*·9-*cis* photoisomerization reaction of retinal in aerated nonpolar solvents has been studied by femtosecond time-resolved ultraviolet-visible (UV-VIS) absorption spectroscopy. The excited-state absorption spectra in the wavelength region 400–800 nm indicate that there is no all-*trans*→13-*cis*·9-*cis* isomerization reaction pathway that is complete in the electronic excited singlet manifold of S_1, S_2, and S_3. The ground-state bleaching recovery of all-*trans* retinal monitored in the near UV (ultraviolet) wavelength region 310–390 nm shows that a perpendicular excited singlet state (p^*) takes part in the all-*trans*→13-*cis*·9-*cis* isomerization reaction. The lifetime of p^* is about 7 ps, and the precursor of p^* is most probably the S_2 state. The isomerization quantum yield derived from the femtosecond UV absorption data agrees well with those determined by the HPLC analysis of the photoproduct. The temperature dependence of the isomerization quantum yield indicates the existence of a potential-energy barrier as high as $(1.2 \pm 0.6) \times 10^3$ cm^{-1} on the reaction pathway from the S_2 state to the p^* state. © *1998 American Institute of Physics.* [S0021-9606(98)00728-4]

I. INTRODUCTION

Retinal, vitamin A aldehyde and the chromophore of light-sensitive proteins known as rhodopsins, is one of the well studied prototypical molecules exhibiting *cis-trans* photoisomerization. The spectroscopic and photochemical properties of retinal strongly depend on its surrounding environment. Though organic solvents appear to provide simpler environments than proteins, the excited electronic structure of retinal in organic solvents seems to be more complicated than that in rhodopsins. Thus, the *cis-trans* photoisomerization reaction mechanism of retinal in organic solvents[1] is much less understood than that in proteins.[2,3] It is of considerable interest to look into the relationship between the excited-state electronic structure and the isomerization pathway/yield of retinal in organic solvents.

Retinal has four C═C double bonds in its polyenic backbone; there are sixteen possible *cis-trans* isomers associated with it including the all-*trans* and four mono-*cis* isomers. It is known that all of these isomers in solution undergo *cis-trans* isomerization upon UV irradiation.[4] In this paper, we focus on the all-*trans*→13-*cis*·9-*cis* isomerization in aerated nonpolar solvents. The quantum yield of the all-*trans*→13-*cis* and the all-*trans*→9-*cis* isomerization upon direct photoexcitation are ~0.1 and ~0.02, respectively.[5,6] Ganapathy and Liu investigated the relation between the photoisomerization quantum yield and the concentration of the all-*trans* isomer by using high performance liquid chromatography (HPLC).[6] They found no concentration dependence of the all-*trans*→13-*cis*·9-*cis* isomerization quantum yield in aerated solutions upon direct photoexcitation. This result indicates that the reaction is unimolecular. Both the excited singlet and triplet states can take part in the photoisomerization. According to our nanosecond time-resolved Raman studies, the photoexcitation of the all-*trans*, 7-*cis*, 9-*cis*, and 11-*cis* isomers in aerated hexane results in an identical Raman spectrum at 20 ns after photoexcitation.[7] This Raman spectrum has been ascribed to the T_1 all-*trans* isomer. Though the 7-*cis*(or 9-*cis*,11-*cis*)→all-*trans* isomerization proceeds via the lowest excited triplet (T_1) manifold, the all-*trans* isomer did not seem to isomerize in the T_1 state (''one-way'' isomerization). This conclusion was supported by subsequent picosecond time-resolved absorption[8] and picosecond 2D-CARS[9] studies. We have recently proved by submicrosecond time-resolved IR (infrared) spectroscopy that there is no isomerization reaction taking place in the T_1 state when the all-*trans* isomer is the starting material.[10] According to our result, T_1 all-*trans* retinal is generated upon direct photoexcitation within the time resolution of the experiment (50 ns) and decays exclusively to the all-*trans* isomer in the ground state (S_0 all-*trans*) with the time constant of 5 μs. The S_0 13-*cis* and S_0 9-*cis* isomers are also generated within the time resolution and do not decay at all. It is concluded that the all-*trans*→13-*cis*·9-*cis* isomerization does not

[a)]Present address: Analytical Sciences Laboratory, Yokohama Research Center, Mitsubishi Chemical Corporation, 1000 Kamoshida, Aoba, Yokohama 227, Japan.
[b)]Author to whom correspondence should be addressed. Electronic mail: hhama@chem.s.u.-tokyo.ac.jp

take place in the T_1 state; in other words, it proceeds via the excited singlet manifold.

Three excited singlet states are known to exist in the low-energy region of all-*trans* retinal up to 30 000 cm^{-1}.[11–21] Though the state ordering is still unclear, there are surely a B_u^+ (π,π^*) state, an A_g^- (π,π^*) state, and an (n,π^*) state in the low-lying excited singlet manifold. Polarized UV-VIS absorption spectroscopic study of crystalline all-*trans* retinal by Drikos *et al.*[12–14] and two-photon fluorescence excitation spectroscopy by Birge *et al.*[16,17] suggested that the lowest excited singlet (S_1) state was of A_g^- (π,π^*) character. On the other hand, fluorescence spectroscopy of hydrogen-bonded retinal by Takemura *et al.* postulated that an (n,π^*) state was the lowest excited singlet state.[11] The kinetics of the excited singlet states have been studied by picosecond time-resolved absorption and fluorescence spectroscopies.[22–24] Our recent femtosecond time-resolved VIS absorption measurement has revealed the presence of two excited singlet states (S_3, S_2) that precede S_1.[25] Larson *et al.* suggested the assignments of the S_3, S_2, and S_1 states to B_u^+ (π,π^*), A_g^- (π,π^*), and (n,π^*), respectively, based on their femtosecond absorption kinetics study.[26] Very recently Takeuchi and Tahara performed femtosecond time-resolved fluorescence up-conversion spectroscopy and found that the transient species of the shortest lifetime emitted the strongest fluorescence. They concluded that the S_3 state of all-*trans* retinal was of B_u^+ (π,π^*) character.[27]

The purpose of this paper is to clarify the all-$trans \rightarrow$13-$cis\cdot$9-cis isomerization mechanism of retinal in aerated nonpolar solvents. The femtosecond time-resolved VIS absorption spectra of all-*trans*, 9-*cis*, and 13-*cis* retinal in hexane have been measured. No *cis* singlet spectra were observed when the all-*trans* isomer was photoexcited. This finding motivated us to perform femtosecond time-resolved absorption spectroscopy in the UV region which can monitor the ground-state recovery of the starting all-*trans* isomer. Two time constants were found in the bleaching recovery of which one was coincident with the T_1 lifetime. The other time constant was longer than the S_2 lifetime but shorter than that of the S_1 state. This time constant of the bleaching recovery is most likely to correspond to the lifetime of a perpendicular excited singlet state. Detailed discussion on the all-$trans \rightarrow$13-$cis\cdot$9-cis isomerization reaction of retinal is presented on the basis of these newly obtained experimental data.

II. EXPERIMENT

Hexane and cyclohexane (HPLC grade) were purchased from Kanto Chemical Co. or Wako Chemical Co. and used as received. All the solvents were aerated. Commercial retinal (Sigma Chemical Co.) was used without further purification. The retinal samples were analyzed for isomeric composition before and after the time-resolved spectroscopic measurements by using HPLC. The isomeric composition of the all-*trans* retinal sample before (and after) the measurements was as follows: all-*trans*, 98.3% (97.5%); 13-*cis*, 1.7% (2.5%). The same quantity of the 13-*cis* retinal sample was as follows: 13-*cis*, 99.2% (97.9%); all-*trans*, 0.5% (1.7%); 9-*cis*, 0.0% (0.1%); 7-*cis*, 0.3% (0.3%).

The femtosecond time-resolved pump–probe UV-VIS absorption spectra of the retinal isomers were measured in the wavelength range 310–390 nm and 400–800 nm by using the femtosecond laser system described elsewhere.[28,29] Hexane or cyclohexane solution (2×10^{-3} mol dm^{-3}, volume 0.2 dm^{-3}) was ejected from a jet nozzle to make a thin flat film suitable for the transient absorption measurements. The solution was photoexcited by the pump pulse at 400 nm with excitation energy density of 2×10 J m^{-2}. The VIS wideband probe was generated by focusing intense 800 nm femtosecond pulses into water. The UV wideband probe was obtained by replacing the 800 nm pulses with the 400 nm. The time resolution was $\sim$0.3 ps both in the VIS and UV wavelength region. A set of time-resolved spectra consisted of 70 time-delay points from -4 to 120 ps. The exposure time of the CCD (charge coupled device) was 1 s, and the number of the exposures at each time delay point was five. A chirp correction was performed by using the optical Kerr effect (OKE) cross-correlation method[29] to make the final time-resolved spectra. The VIS absorption measurements were done at 293 ± 2 K. As will be described later, the all-$trans \rightarrow$13-$cis\cdot$9-cis isomerization total quantum yield is obtained from the femtosecond UV absorption data. In order to investigate the temperature dependence of the quantum yield, the solution temperature in the UV absorption measurements was set at four different points: 269, 273, 293, and 298 ± 2 K.

III. RESULTS

A. Femtosecond time-resolved VIS absorption spectra

In Fig. 1, fourteen representative femtosecond time-resolved VIS absorption spectra of all-*trans* retinal in aerated hexane are shown. The spectra are shown in the forms of difference spectra. The positive signals correspond to the photoinduced increase of absorbance which is caused by transitions from excited states to higher excited states. The negative signals correspond to the photoinduced decrease of absorbance which is caused by ground-state bleaching and/or stimulated emission gain. Stimulated Raman loss (inverse Raman) may also contribute to the positive signals and stimulated Raman gain to the negative signals.

There are several salient features in the time-resolved spectra in Fig. 1. First of all, the absorption band around 450 nm at 100 ps after the photoexcitation is very distinct and undoubtedly assigned to the $T_n \leftarrow T_1$ absorption.[8,25,30,31] As mentioned in Sec. I, the T_1 species has exclusively the all-*trans* configuration when the S_0 all-*trans* isomer is the starting material.[7–10,31] The absorption band around 450 nm in Fig. 1 is ascribed to the T_1 all-*trans* isomer. The band shape and the peak position of this band agree well with those in the literature.[8,30,32,33] Broad absorption bands in the subpicosecond time range are other features to be noted in the spectra in Fig. 1. These bands of all-*trans* retinal were observed first by Hochstrasser *et al.* in 1976,[22] and there was no fur-

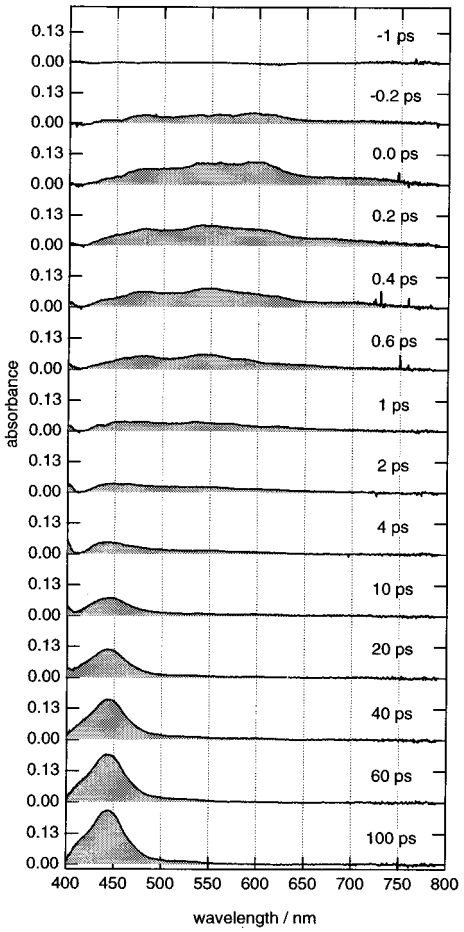

FIG. 1. Femtosecond time-resolved VIS absorption spectra of all-*trans* retinal in hexane at various time delays.

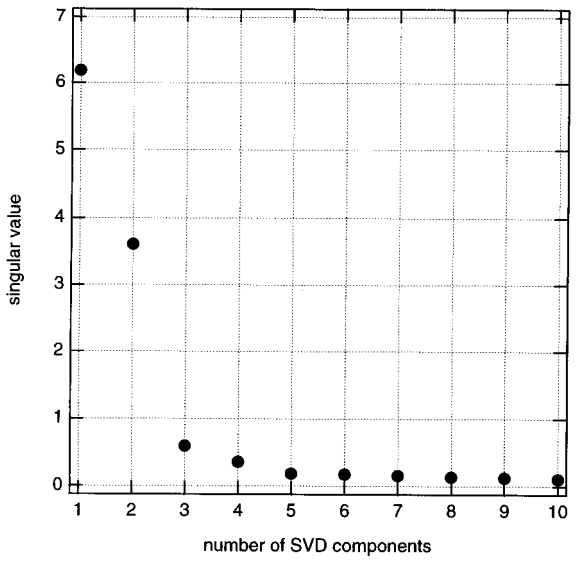

FIG. 2. Singular values obtained from the SVD analysis of the time-resolved VIS spectra of all-*trans* retinal in hexane.

ther report until our letter was published in 1996.[25] It is likely that the excited singlet states contribute to these broad bands, but no definitive assignments have been performed. A detailed kinetics analysis is necessary to obtain more insight into the singlet electronic structure of retinal from the time-resolved spectra in Fig. 1.

When two or more transient species are involved in one set of time-resolved spectra just like the present case, the singular value decomposition (SVD) analysis combined with fitting procedures is often useful for its kinetics analysis. The methods and the advantages of the SVD analysis have been briefly reviewed by Chen and Braiman[34] and there have been many examples in various fields which show the usefulness of SVD.[10,25,35–38] In SVD, a set of time-resolved spectra is treated as a matrix. Let this matrix be written as **A** of which the ith row vector corresponds to the spectrum at the ith time delay point. The SVD analysis yields several SVD components from **A**, and each SVD component has its singular value (scalar), its spectrum (column vector), and its temporal evolution (column vector). **A** is expressed as follows:

$$\mathbf{A}=\sum_{i=1} V_i \mathbf{t}_i {}^t\mathbf{s}_i , \tag{1}$$

where V_i is the singular value of the ith SVD component, $\mathbf{s}_i$ is the spectrum of the ith SVD component, and $\mathbf{t}_i$ is the temporal evolution of the ith SVD component. All the singular values are positive, and $V_i > V_j$ if $i<j$. $\{\mathbf{s}_i\}$ and $\{\mathbf{t}_i\}$ are both normalized orthogonal sets; ${}^t\mathbf{s}_i\mathbf{s}_j=\delta_{ij}$ and ${}^t\mathbf{t}_i\mathbf{t}_j=\delta_{ij}$. In Eq. (1), the contribution of the ith SVD component to **A** is determined by V_i. SVD components with smaller singular values are less significant. We have only to take into account the SVD components having large singular values. The omission of the SVD components with small singular values is effective in simplifying the analysis and removing noise. This is one of the advantages of the SVD analysis.

The SVD of the set of the time-resolved spectra in Fig. 1 yielded four principal singular values as shown in Fig. 2. The fifth and the higher singular values were almost zero and regarded as noise. In order to obtain physically meaningful temporal evolutions and the corresponding spectra from the SVD components, we start with the following kinetics scheme for the photophysics of all-*trans* retinal:

$$S_0 \xrightarrow[h\nu]{} S_3 \xrightarrow{\phi_3\gamma_3} S_2 \xrightarrow{\phi_2\gamma_2} S_1 \xrightarrow{\phi_1\gamma_1} T_1 . \tag{I}$$

Here it is assumed that only the $S_3 \leftarrow S_0$ transition is one-photon allowed. This assumption is based on the results of femtosecond time-resolved fluorescence up-conversion spectroscopy by Takeuchi and Tahara.[27] According to their conclusion, the S_3 state of all-*trans* retinal is of B_u^+ (π,π^*) character and the $S_3 \leftarrow S_0$ transition contribute to about 96% of the ground-state absorption. The contribution of the direct $S_2 \leftarrow S_0$ photoexcitation is small and disregarded in the present analysis.[39] The simplest relaxation schemes are assumed among the three excited singlet states: The S_3 state relaxes to the S_2 state with the quantum efficiency ϕ_3 and the lifetime γ_3^{-1}, S_2 to S_1 with ϕ_2 and γ_2^{-1}, and S_1 to T_1 with ϕ_1 and γ_1^{-1}. Since the maximum time delay after the photoexcitation in the present experiments is about 100 ps, it is unnecessary to take into account the relaxation of the T_1

state.[9] According to Kinetics Scheme (I), the time-delay dependence of the population of each electronic state is expressed as follows:

$$[S_3]=e^{-\gamma_3 t}, \tag{2}$$

$$[S_2]=\frac{\phi_3\gamma_3}{\gamma_3-\gamma_2}\,(e^{-\gamma_2 t}-e^{-\gamma_3 t}), \tag{3}$$

$$[S_1]=\frac{\phi_2\phi_3\gamma_2\gamma_3}{(\gamma_2-\gamma_1)(\gamma_3-\gamma_1)}\left(e^{-\gamma_1 t}-\frac{\gamma_3-\gamma_1}{\gamma_3-\gamma_2}e^{\gamma_2 t}+\frac{\gamma_2-\gamma_1}{\gamma_3-\gamma_2}\,e^{-\gamma_3 t}\right), \tag{4}$$

$$[T_1]=\phi_1\phi_2\phi_3\left\{1-\frac{\gamma_2\gamma_3 e^{-\gamma_1 t}}{(\gamma_2-\gamma_1)(\gamma_3-\gamma_1)}+\frac{\gamma_1\gamma_3 e^{-\gamma_2 t}}{(\gamma_2-\gamma_1)(\gamma_3-\gamma_2)}-\frac{\gamma_1\gamma_2 e^{-\gamma_3 t}}{(\gamma_3-\gamma_1)(\gamma_3-\gamma_2)}\right\}, \tag{5}$$

where δ-function-like photoexcitation at $t=0$ is assumed and the S_3 population directly generated by the photoexcitation is set to be unity. All the populations are zero for $t<0$. There is a relation among the populations of the five electronic states involved in Kinetics Scheme (I):

$$[S_0]=-[S_3]-[S_2]-[S_1]-[T_1], \tag{6}$$

where the S_0 population $[S_0]$ is always negative. The term ''population'' in this paper stands for the difference between the population with and without photoexcitation. Though the five electronic states are involved in Kinetics Scheme (I), four SVD components are enough because $[S_0]$ is expressed as a linear combination of the other four populations. The number of SVD components that have to be taken into account does not always coincide with that of transient species, since all the populations of transient species are not always linearly independent just like the present case, while all the temporal behaviors of SVD components have to be linearly independent.

We now derive the populations and the spectra of the transient species (S_3,S_2,S_1,T_1) from $\{\mathbf{t}_i\}_{1\leqslant i\leqslant 4}$ and $\{\mathbf{s}_i\}_{1\leqslant i\leqslant 4}$ of the SVD components: The product of the ith singular value and the temporal evolution of the ith SVD component, $V_i\mathbf{t}_i$, is fitted to the following model function:

$$c_{i4}[S_3]+c_{i3}[S_2]+c_{i2}[S_1]+c_{i1}[T_1], \tag{7}$$

of which the fitting parameters are $\gamma_1,\gamma_2,\gamma_3,c_{i1},c_{i2},c_{i3},c_{i4}$. The parameters $\gamma_1,\gamma_2,\gamma_3$ have to be common to all the four SVD components. The quantum efficiencies, ϕ_1,ϕ_2,ϕ_3, are not determined by the fitting procedure. In the practical fitting procedure, the model function of Eq. (7) is convoluted with a Gaussian function which represents the instrumental response. The relation between $\{\mathbf{t}_i\}_{1\leqslant i\leqslant 4}$ and the populations of the transient species is expressed by using the converged fitting parameters c_{ij} as follows:

$$\begin{pmatrix} V_1{}^t\mathbf{t}_1\\ V_2{}^t\mathbf{t}_2\\ V_3{}^t\mathbf{t}_3\\ V_4{}^t\mathbf{t}_4\end{pmatrix}=\mathbf{C}\begin{pmatrix} {}^t\mathbf{T}_{1pop}\\ {}^t\mathbf{S}_{1pop}\\ {}^t\mathbf{S}_{2pop}\\ {}^t\mathbf{S}_{3pop}\end{pmatrix}. \tag{8}$$

where $\mathbf{C}$ is a matrix whose (i,j) component is c_{ij}, $\mathbf{S}_{3pop}$ is a column vector whose ith component is the $\mathbf{S}_3$ population at the ith time delay point, and so are $\mathbf{S}_{2pop}$, $\mathbf{S}_{1pop}$, $\mathbf{T}_{1pop}$. The populations of the transient species are finally recomposed from $\{\mathbf{t}_i\}_{1\leqslant i\leqslant 4}$ as follows:

$$\begin{pmatrix} {}^t\mathbf{T}_{1pop}\\ {}^t\mathbf{S}_{1pop}\\ {}^t\mathbf{S}_{2pop}\\ {}^t\mathbf{S}_{3pop}\end{pmatrix}=\mathbf{C}^{-1}\begin{pmatrix} V_1{}^t\mathbf{t}_1\\ V_2{}^t\mathbf{t}_2\\ V_3{}^t\mathbf{t}_3\\ V_4{}^t\mathbf{t}_4\end{pmatrix}. \tag{9}$$

The spectra of the transient species have to satisfy the following equation:

$$\mathbf{A}=\mathbf{S}_{3pop}{}^t\mathbf{S}_{3spe}+\mathbf{S}_{2pop}{}^t\mathbf{S}_{2spe}+\mathbf{S}_{1pop}{}^t\mathbf{S}_{1spe}+\mathbf{T}_{1pop}{}^t\mathbf{T}_{1spe}, \tag{10}$$

where $\mathbf{S}_{3spe}$ is a column vector and stands for the absorption spectrum of the $\mathbf{S}_3$ state. The ith component of $\mathbf{S}_{3spe}$ corresponds to absorbance at the ith wavelength point, and the same for $\mathbf{S}_{2spe}$, $\mathbf{S}_{1spe}$, and $\mathbf{T}_{1spe}$. By using Eqs. (1), (9), and (10), the spectra of the transient species are recomposed from $\{\mathbf{s}_i\}_{1\leqslant i\leqslant 4}$

$$\begin{pmatrix} {}^t\mathbf{T}_{1spe}\\ {}^t\mathbf{S}_{1spe}\\ {}^t\mathbf{S}_{2spe}\\ {}^t\mathbf{S}_{3spe}\end{pmatrix}={}^t\mathbf{C}\begin{pmatrix} {}^t\mathbf{s}_1\\ {}^t\mathbf{s}_2\\ {}^t\mathbf{s}_3\\ {}^t\mathbf{s}_4\end{pmatrix}. \tag{11}$$

The SVD analysis of the 70 time-resolved spectra of all-*trans* retinal in hexane gives the absorption spectra and the population changes shown in Figs. 3(a)–3(h). In the analysis, ϕ_2 was fixed to 0.74, and ϕ_1 and ϕ_3 were put equal to unity. Note that the triplet quantum yield (which is equal to $\phi_1\phi_2\phi_3$) of all-*trans* retinal in hexane at room temperature is going to be determined later in this paper to be 0.74. It is also shown later that ϕ_1 is equal to one. Nearly identical spectra and populations were also obtained in the case of all-*trans* retinal in cyclohexane. This means that hexane and cyclohexane provide similar environments for the excited-state dynamics of retinal. Time constants obtained from twelve independent measurements and analyses are given in Table I.

The spectrum in Fig. 3(d) is identical with the known $T_n\leftarrow T_1$ absorption spectrum of all-*trans* retinal in nonpolar solvents.[8,25,30–33] The T_1 lifetime is much longer than 100 ps and is fixed to infinity in the fitting procedures. The spectrum in Fig. 3(c) corresponds to the $S_n\leftarrow S_1$ absorption spectrum, though the band shape looks strange. It will be shown later that the main band of the $S_n\leftarrow S_1$ absorption lies in the wavelength range 350–400 nm, and only the band edge appears in Fig. 3(c). The S_1 lifetime, 32 ± 2 ps, agrees well with the literature values.[8,22,24] It also agrees with the T_1 rise time, indicating that the S_1 state is the precursor of the T_1 all-*trans* isomer and that the S_1 state is most likely to be in the all-*trans* configuration. The S_1 rise time, which is equal to the

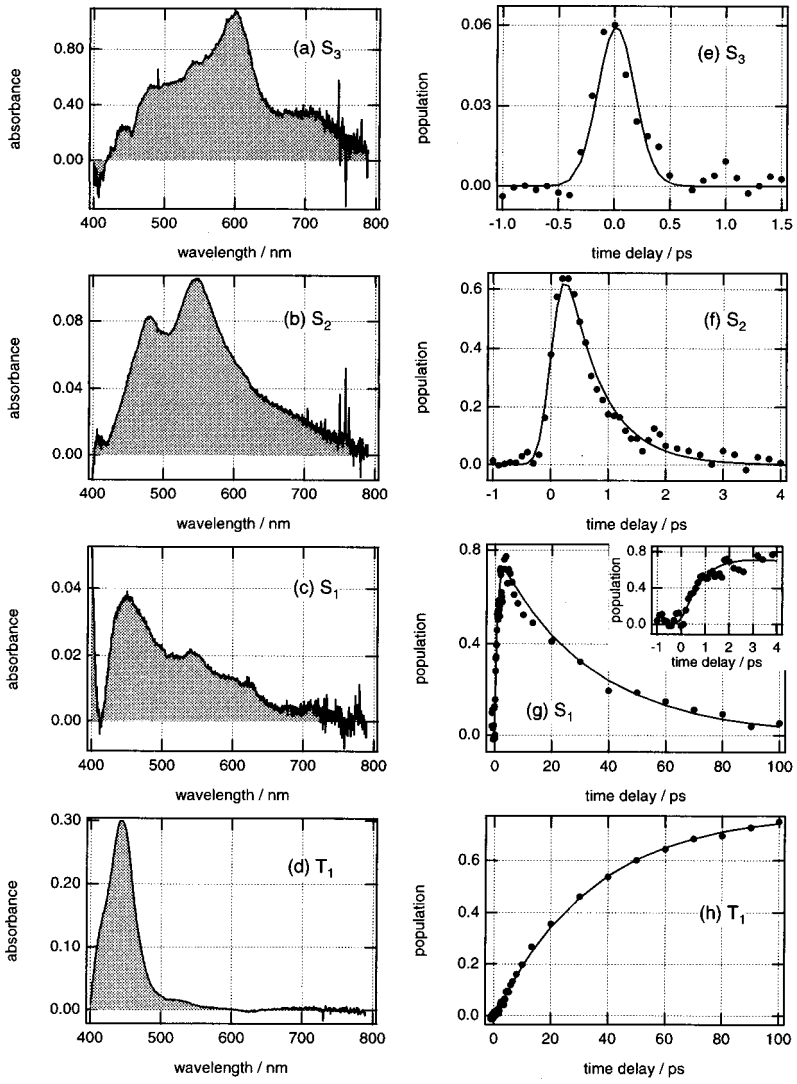

FIG. 3. Spectra [(a)–(d)] and populations [(e)–(h)] of the four transient species obtained from the time-resolved VIS spectra of all-*trans* retinal in hexane.

S_2 lifetime, is obtained as 0.73 ± 0.2 ps. This value is smaller than the value reported in our previous letter (1.2 ps)[25] and that recently reported by Larson *et al.* (1.8 ps),[26] but larger than that determined by Takeuchi and Tahara (0.37 ± 0.02 ps) using the fluorescence up-conversion technique.[27] In our previous letter, only three SVD components were taken into account because of a lower signal to noise ratio and a narrower wavelength range measured.[25] An exponential time constant in the SVD analysis is strongly influenced by the number of components.[34] We believe that the present value is more reliable than the previous one. We have no clear idea why the S_2 lifetime in the present study does not agree with that in the fluorescence up-conversion study[27] even if experimental errors are taken into account. The transient species exhibiting the spectrum in Fig. 3(b) and the population change in Fig. 3(f) is the precursor of S_1 all-*trans* retinal and is naturally assigned to the S_2 all-*trans* isomer. The broad absorption bands in the subpicosecond time region in Fig. 1 is due to the $S_n \leftarrow S_2$ absorption spectrum. The S_2 rise time or the S_3 lifetime is too short to be determined by the present analysis. It is fixed to the value, 0.03 ps, reported by Takeuchi and Tahara.[27] This means that we have no clear evidence in the present study that the S_2 state is generated only from the S_3 state, as assumed in Kinetics Scheme (I). There remains a possibility that some portion of the S_2 population is directly generated by the photoexcitation. The spectrum in Fig. 3(a) is assigned to the $S_n \leftarrow S_3$ absorption spectra. The band shape of the $S_n \leftarrow S_3$ absorption is distinct from that of the $S_n \leftarrow S_2$ absorption. The vibrationally excited S_2 state (S_2^*) does not seem to contribute to the absorption band in Fig. 3(a). Note that vibrational excitation most often causes only broadening of an absorption

TABLE I. Excited-state lifetimes of all-*trans* retinal in hexane at 293 K obtained from the fetosecond time-resolved VIS absorption spectra.

State	Lifetime
S_3	0.03 ps (fixed)
S_2	0.73 ± 0.2 ps
S_1	32 ± 2 ps
T_1	∞ (fixed)

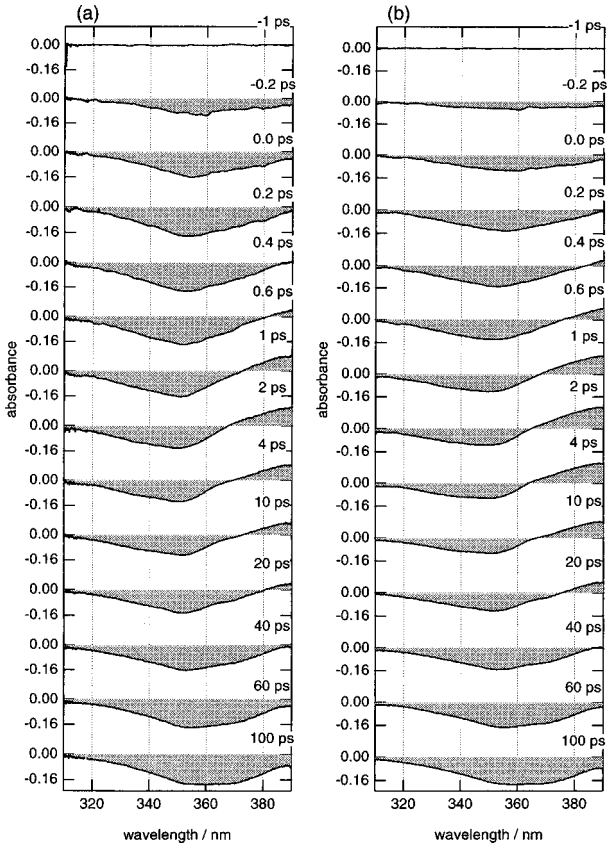

FIG. 4. Femtosecond time-resolved UV absorption spectra of all-*trans* retinal in hexane at various time delays at (a) 298 K and (b) 269 K.

band.[28,40,41] The small negative band at wavelength 454 nm in Fig. 3(a) is the impulsive stimulated Raman gain signal assigned to the CH stretching modes of hexane. The Raman gain process is also instantaneous in the present time resolution and has the same temporal evolution as that of the S_3 population. Two possibilities are considered for the negative signals around 407 nm in Fig. 3(a); the ground-state bleaching or the stimulated emission gain. It will be shown later in the femtosecond time-resolved UV spectra that negative signals due to the ground-state bleaching is not expected to be large in the wavelength range longer than 400 nm. Therefore, the stimulated emission gain is more likely than the ground-state bleaching.

B. Femtosecond time-resolved UV absorption spectra

Fourteen representative femtosecond time-resolved UV absorption spectra of all-*trans* retinal in hexane at 298 K and those at 269 K are shown in Figs. 4(a) and 4(b), respectively. The femtosecond time-resolved absorption spectra in the near UV region are reported for the first time to the best of our knowledge. Since the ground-state absorption bands of all-*trans* retinal exist in the wavelength range 310–390 nm, we expect that negative signals due to the ground-state bleaching dominate the spectra. The bleaching band shape at 100 ps after the photoexcitation is in agreement with that measured by Veyret *et al.* with nanosecond time resolution.[33] In the time range 0.6–20 ps, positive signals are observed in the wavelength range longer than 370 nm. Similar measurements were performed with a cyclohexane solution at 293 K which gave nearly identical spectra with those in hexane at 298 K. This once again confirms our idea that hexane and cyclohexane give similar environments for all-*trans* retinal in the excited electronic states.

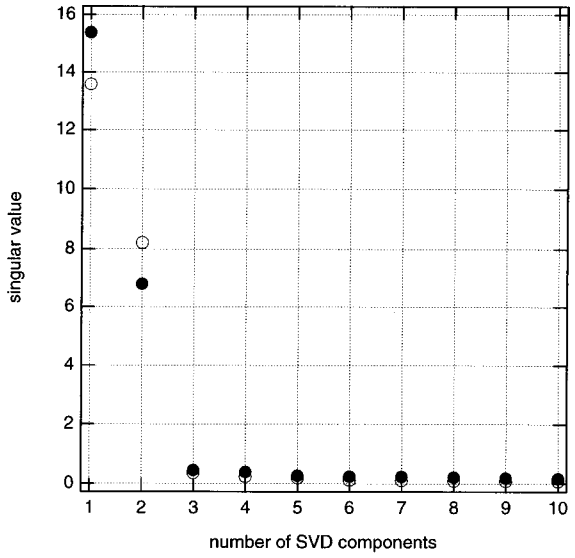

FIG. 5. Singular values obtained from the SVD analysis of the time-resolved UV spectra of all-*trans* retinal in hexane at 298 K (solid circles) and 269 K (open circles).

The SVD analysis of the femtosecond time-resolved UV absorption spectra in Figs. 4(a) and 4(b) gave two series of singular values as shown in Fig. 5. We recognize two principal singular values in both of these two series. The third and higher SVD components are disregarded. As shown above, the time-resolved VIS absorption spectra of all-*trans* retinal have been successfully interpreted in terms of Kinetics Scheme (I). The five transient species of which four are linearly independent are involved in Kinetics Scheme (I). It is now necessary to identify the two transient species that contribute to the time-resolved UV spectra. One is definitely the S_0 state, because the negative signals in Fig. 4 must be due to the ground-state bleaching. The other is most likely to be the S_1 state which has a 32 ps lifetime that corresponds to the observed positive signals. The fitting of the two principal temporal evolutions of the SVD components were carried out as in the case of the VIS spectra. It turned out that the fitting was successful only when the following model functions were assumed for the S_1 and S_0 populations:

$$f_{S1}(t) = e^{-\gamma_1 t} - e^{-\gamma_2 t}, \tag{12}$$

$$f_{S0}(t) = -1 - Ae^{-\gamma_p t}. \tag{13}$$

Equation (12) is derived from Eq. (4) by using the relation $\gamma_3 \gg \gamma_2$. The physical meaning of Eq. (13) and the new parameters A and γ_p will be discussed later.

Figure 6 shows the spectra and the population changes of the S_1 and S_0 states of all-*trans* retinal in hexane at 298 K obtained by the SVD analysis of the spectra in Fig. 4(a). The three time constants $(\gamma_2^{-1}, \gamma_1^{-1}, \gamma_p^{-1})$ and the parameter A determined from eight independent measurements are as follows: $\gamma_2^{-1} = 0.56 \pm 0.05$ ps, $\gamma_1^{-1} = 31 \pm 3$ ps, $\gamma_p^{-1} = 7.2$

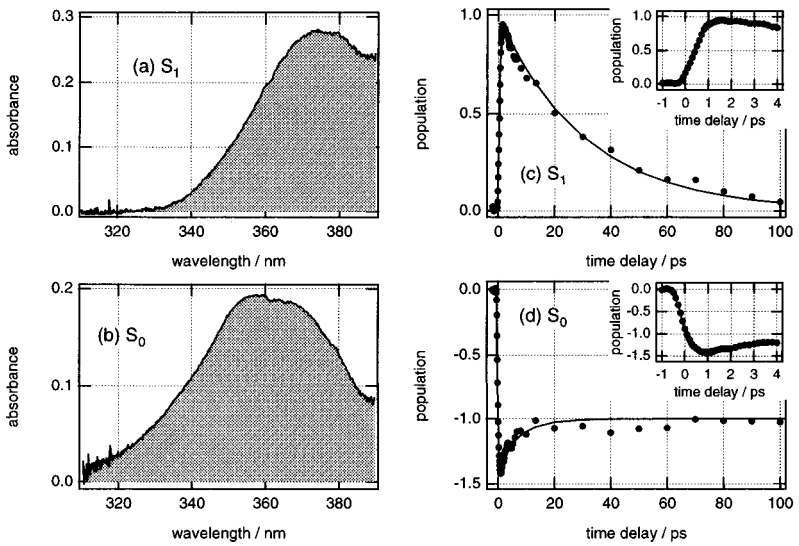

FIG. 6. Spectra [(a) and (b)] and populations [(c) and (d)] of the two transient species obtained from the time-resolved UV spectra of all-*trans* retinal in hexane at 298 K.

± 2 ps, $A=0.36\pm 0.08$. The two time constants, γ_2^{-1} and γ_1^{-1}, are in good agreement with those determined from the VIS spectra within experimental uncertainties. It is confirmed that the transient species showing the spectrum in Fig. 6(a) and the population in Fig. 6(c) is the same S_1 all-*trans* isomer as that identified in the analysis of the VIS data. As seen from Fig. 6(a), a strong $S_n \leftarrow S_1$ absorption is located in the wavelength range 360–390 nm. The negative population in Fig. 6(d) is ascribed to the ground-state bleaching. Though the instantaneous decrease of the S_0 population in Fig. 6(d) is consistent with the depletion of the S_0 all-*trans* isomer by the photoexcitation, its recovery with the time constant of 7.2 ps ($=\gamma_p^{-1}$) has to be accounted for. The most simple and reasonable modification of Kinetics Scheme (I) is to assume that an intermediate having a lifetime γ_p^{-1} exists and that it exclusively decays to S_0. The symbol p^* is hereafter used to designate this intermediate. As discussed later, the p^* state is considered to be the ''perpendicular excited singlet state'' which plays an essential role in the process of isomerization. Either the S_3 or the S_2 state can be the precursor of p^*, since the lifetime of p^* (γ_p^{-1}) is longer than those of S_3 and S_2 but is shorter than those of S_1 and T_1. Here we assume that the S_2 state is the precursor of p^*. This is to assume that the isomerization proceeds from the S_2 state. Then, we need to add to Kinetics Scheme (I) an extra relaxation pathway of the S_2 state

$$S_0 \xrightarrow[h\nu]{} S_3 \xrightarrow{\gamma_3} S_2 \xrightarrow{\phi_2\gamma_2} S_1 \xrightarrow{\gamma_1} T_1$$

$$S_2 \xrightarrow{(1-\phi_2)\gamma_2} p^* \xrightarrow{\gamma_p} S_0. \qquad \text{(II)}$$

The S_0 and p^* populations in Kinetics Scheme (II) are given as follows:

$$[S_0]=-[S_3]-[S_2]-[S_1]-[T_1]-[p^*], \qquad (14)$$

$$[p^*]=\frac{(1-\phi_2)\gamma_2\gamma_3}{(\gamma_2-\gamma_p)(\gamma_3-\gamma_p)}\left(e^{-\gamma_p t}-\frac{\gamma_3-\gamma_p}{\gamma_3-\gamma_2}e^{-\gamma_2 t}+\frac{\gamma_2-\gamma_p}{\gamma_3-\gamma_2}e^{-\gamma_3 t}\right). \qquad (15)$$

By substituting Eqs. (2)–(5) and (15) for Eq. (14) and using the relations $\gamma_3 \gg \gamma_p$ and $\gamma_2 \gg \gamma_p$, Eq. (14) is reduced to Eq. (13). Thus, the kinetics assumed in the SVD analysis of the UV absorption spectra, Eqs. (12) and (13), are derived from Kinetics Scheme (II). We also have a relation between ϕ_2 and A as follows:

$$\phi_2=\frac{1}{1+A}. \qquad (16)$$

The S_1 and T_1 quantum yields are given by $1/(1+A)$, and that of p^* by $A/(1+A)$. There is no $S_1 \rightarrow S_0$ relaxation pathway ($\phi_1=1$) as indicated by the constant S_0 population for $t>20$ ps.

The SVD analyses of the femtosecond UV spectra of all-*trans* retinal in hexane at lower temperatures were performed in similar ways. It was found in the actual fitting procedures that γ_p was nearly independent of temperature while A was not. Both γ_p and A were determined by a small fraction of the data in the time range 0–20 ps [see Fig. 6(d)], and it was not possible to determine these two quantities simultaneously with small uncertainties. Therefore, γ_p^{-1} was fixed to 7.2 ps in order to determine the temperature dependence of A as exact as possible. The spectra and the populations of the S_1 and S_0 all-*trans* species in hexane at 269 K are shown in Fig. 7. The amplitude A of the S_0 recovery in Fig. 7(d) is much smaller than that in Fig. 6(d). The S_1 decay in Fig. 7(c) is slower than that in Fig. 6(c). The converged values of the fitting parameters, γ_2^{-1}, γ_1^{-1}, A, obtained from several independent measurements at four temperatures are given in Table II.

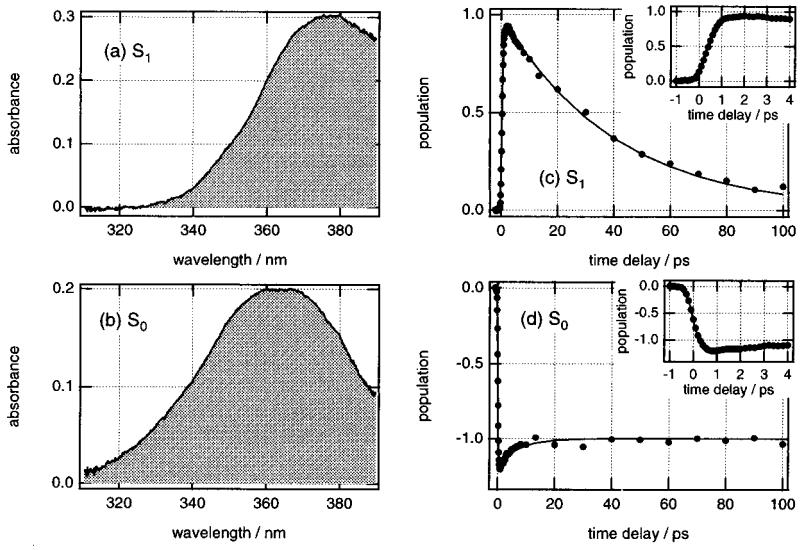

FIG. 7. Spectra [(a) and (b)] and populations [(c) and (d)] of the two transient species obtained from the time-resolved UV spectra of all-*trans* retinal in hexane at 269 K.

IV. DISCUSSION

All the femtosecond time-resolved spectra, both in the VIS and UV wavelength regions, have been successfully interpreted by the SVD analysis based on Kinetics Scheme (II). This scheme is fully consistent with the assignment of the S_3 state to B_u^+ (π,π^*) which was recently verified by femtosecond time-resolved fluorescence up-conversion spectroscopy.[27] The other two excited singlet states, S_2 and S_1, are most likely to be A_g^- (π,π^*) and (n,π^*), respectively. It has been shown by an electron spin echo experiment that the T_1 state of all-*trans* retinal is of (π,π^*) character.[42] The very fast $S_1 \rightarrow T_1$ intersystem crossing (32 ps) is indicative of a direct process $^1(n,\pi^*) \rightarrow {}^3(\pi,\pi^*)$, suggesting that the S_1 state is of (n,π^*) character. The S_2 state is then considered to be of A_g^- (π,π^*) character.

Kinetics Scheme (I) starts from the S_0 state with the all-*trans* configuration and ends with the T_1 state having the same configuration. It is, therefore, natural to assume that the three excited singlet states have also the all-*trans* configuration. In order to check whether other *cis* excited states are involved in the all-*trans* VIS spectra (Fig. 1) as minor components, the products of the spectra and the populations of the S_3, S_2, S_1, and T_1 states (Fig. 3) were subtracted from the raw all-*trans* VIS spectra. The resultant residual spectra are shown in Fig. 8 together with the raw femtosecond time-resolved VIS absorption spectra of 13-*cis* retinal in hexane. There are no meaningful bands in the residual spectra, showing that the femtosecond time-resolved VIS absorption spectra of all-*trans* retinal are fully explained by Kinetics Scheme (I). This means that no 13-*cis* excited-state species as a photoisomerization product is observed in the all-*trans* VIS spectra. We have no evidence for the all-*trans* $\rightarrow$13-*cis*·9-*cis* photoisomerization pathway that is complete in the electronic excited states. It is, therefore, necessary to figure out another reaction mechanism that is not complete in the excited singlet states.

TABLE II. Converged fitting parameters in the analyses of the femtosecond time-resolved UV absorption spectra of all-*trans* retinal in aerated nonpolar solvents at four different temperatures.

Temperature/K	S_2 lifetime/ps	S_1 lifetime/ps	A
298	0.56±0.05	31±3	0.36±0.08
293	0.47±0.05	31±1	0.29±0.04
273	0.53±0.05	42±2	0.21±0.01
269	0.49±0.02	42±1	0.18±0.02

Now we consider an isomerization scheme shown in Fig. 9, which involves the p^* state as the key intermediate. In this scheme, the isomerization proceeds from the S_2 state to the perpendicular excited singlet state, p^*, which finally gives the *trans* and *cis* isomers in the ground state in a nearly 50/50 ratio. The isomerization scheme shown in Fig. 9 is fully consistent with Kinetics Scheme (II) as will be shown later. All-*trans* retinal in nonpolar solvents undergoes isomerization to both the 13-*cis* and 9-*cis* isomers. Therefore, strictly speaking, we should consider two different perpendicular configurations of which one is twisted about the C_{13}═C_{14} double bond and the other about the C_9═C_{10} double bond. However it is sufficient to assume only the former perpendicular state because (i) the 13-*cis* quantum yield is about 5–10 times higher than the 9-*cis* quantum yield, and (ii) the signal to noise ratio in the present femtosecond time-resolved UV absorption data is not sufficient to assume two different perpendicular states with different lifetimes. Therefore, the isomerization scheme in Fig. 9 does not distinguish the 13-*cis* and 9-*cis* isomers. The reaction mechanism is then the same as that of the *trans*$\rightarrow$*cis* photoisomerization of stilbene. The p^* state decays to the perpendicular ground state, p, which is then deactivated to give the *trans* and *cis* isomers in the ground state in a 50/50 ratio. The decay rate of p is assumed to be much larger than that of p^*, $(7.2\ \text{ps})^{-1}$. The lifetime of the perpendicular excited singlet state of stilbene is thought to be much shorter than a picosecond[43–45] while that of *trans*-1, 1′-biindanylidene

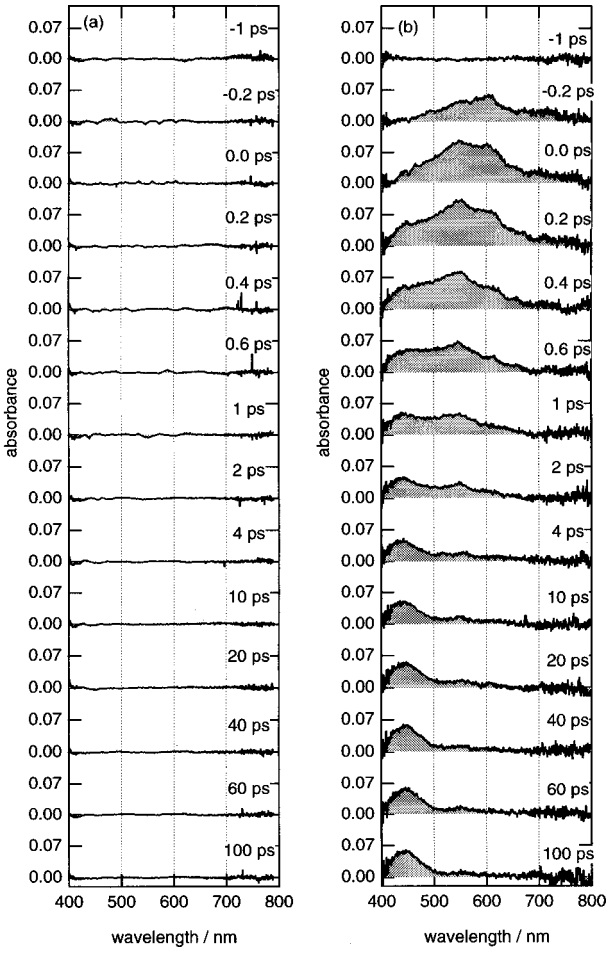

FIG. 8. (a) Residual spectra of all-*trans* retinal in hexane at various time delays obtained by subtracting the contribution of the four transient species in Fig. 3 from the raw spectra in Fig. 1. (b) Femtosecond time-resolved VIS absorption spectra of 13-*cis* retinal in hexane at various time delays.

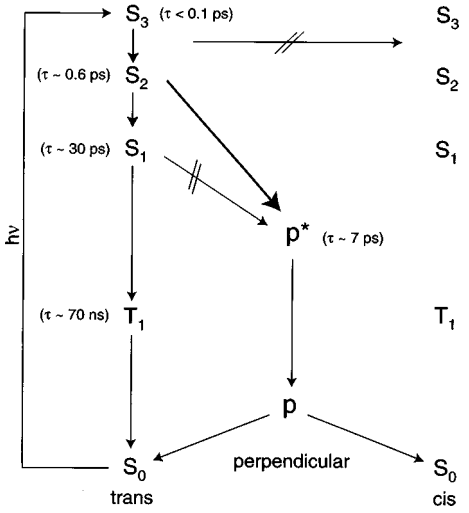

FIG. 9. All-*trans*→mono-*cis* photoisomerization reaction scheme of retinal in aerated nonpolar solvents.

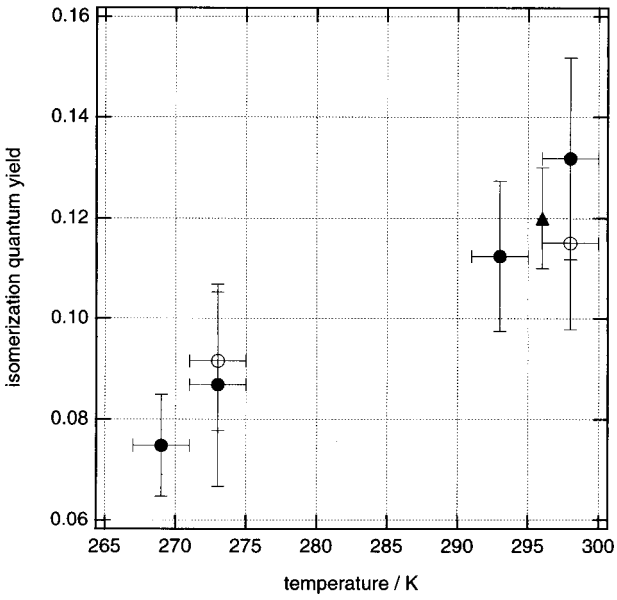

FIG. 10. Temperature dependence of all-*trans*→13-*cis*·9-*cis* photoisomerization total quantum yield obtained from the femtosecond UV data (solid circles). The isomerization quantum yields upon direct photoexcitation measured by HPLC are shown together: Open circles, W. H. Waddell and K. Chihara (Ref. 5); solid triangle, S. Ganapathy and R. S. H. Liu (Ref. 6).

(stiff stilbene) is about 10 ps.[46] The excited singlet state of tetraphenylethylene, for which the perpendicular configuration is confirmed by nanosecond time-resolved Raman spectroscopy,[47] has a lifetime of 3 ns.[48] The 7 ps lifetime of the p^* state of retinal is well in the range of the reported lifetimes of the excited singlet perpendicular states of olefins.

According to the isomerization scheme in Fig. 9, the total quantum yield of the all-*trans*→13-*cis*·9-*cis* photoisomerization, ϕ_{iso}, can be derived from the femtosecond UV data as follows:

$$\phi_{iso}=\frac{1}{2}\cdot\frac{A}{1+A}. \tag{17}$$

Note that ϕ_{iso} is half of the quantum yield of p^*. The temperature dependence of the all-*trans*→13-*cis*·9-*cis* photoisomerization total quantum yield is obtained from Eq. (17) and Table II as shown in Fig. 10. The total quantum yields upon direct photoexcitation measured by HPLC[5,6] are also shown together. The total quantum yields at the four different temperatures obtained in the present time-resolved spectroscopic measurements agree well with the literature values. This agreement strongly supports the present isomerization scheme in Fig. 9.

The same S_0 recovery kinetics [Eq. (13)] is obtained if we assume that the S_3 state rather than the S_2 state is the precursor of p^*. This means that we cannot unequivocally determine the isomerization pathway solely from the present femtosecond UV data. However, the fact that the isomerization quantum yield decreases with decreasing temperature means that thermal excitations are involved in the process of the p^* formation. The S_3 lifetime, which has been reported as 0.03 ps,[27] is too short to be associated with any kind of

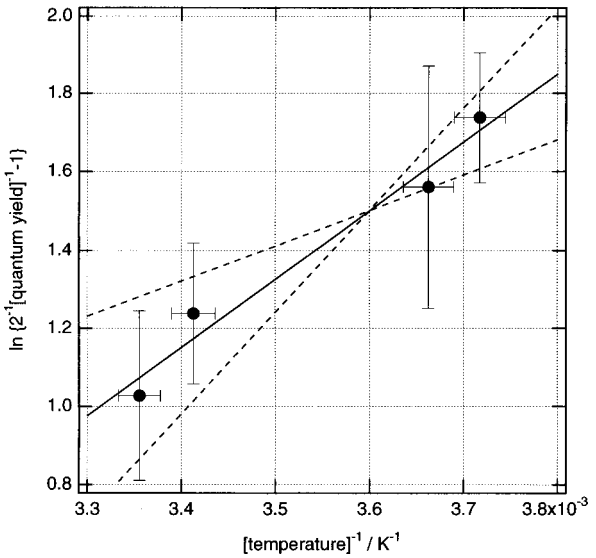

FIG. 11. Arrhenius plot to obtain the activation energy of all-*trans* $\rightarrow$13-*cis*·9-*cis* isomerization. Two dashed lines correspond to the error range of the activation energy.

thermal excitations. It is considered that the precursor of p^* is the S_2 state. Then, the total quantum yield is determined by two rate constants in the following way:

$$\phi_{iso}=\frac{1}{2}\cdot\frac{\gamma_{2\rightarrow p^*}}{\gamma_{2\rightarrow 1}+\gamma_{2\rightarrow p^*}}, \tag{18}$$

where $\gamma_{2\rightarrow 1}$ is the $S_2\rightarrow S_1$ internal conversion rate constant and $\gamma_{2\rightarrow p^*}$ is the $S_2\rightarrow p^*$ decay rate constant, and the equation $\gamma_2=\gamma_{2\rightarrow 1}+\gamma_{2\rightarrow p^*}$ has to be satisfied. The temperature dependence of ϕ_{iso} in Fig. 10 means that $\gamma_{2\rightarrow p^*}$ decreases as the temperature decreases. The most straightforward way to introduce the temperature dependence of $\gamma_{2\rightarrow p^*}$ is to use a transition-state expression as follows:

$$\gamma_{2\rightarrow p^*}=a_{2\rightarrow p^*}\exp\left(-\frac{E_a}{k_BT}\right), \tag{19}$$

where $a_{2\rightarrow p^*}$ is the rate at a high-temperature limit, E_a is an activation energy, and T is temperature. On the assumption that $\gamma_{2\rightarrow 1}$ is independent of T, an Arrhenius-type relation is obtained by using Eqs. (18) and (19):

$$\log\left(\frac{1}{2\phi_{iso}}-1\right)=\frac{E_a}{k_BT}+\log\left(\frac{\gamma_{2\rightarrow 1}}{a_{2\rightarrow p^*}}\right). \tag{20}$$

Plotting $\log(2^{-1}\phi_{iso}^{-1}-1)$ versus T^{-1} as shown in Fig. 11, we obtain E_a as $(1.2\pm 0.6)\times 10^3$ cm^{-1} (14 ± 7 kJ mol^{-1}). The data of Waddell and Chihara gave 7.6×10^2 cm^{-1}. The present E_a value is similar to the activation energy for the *trans*$\rightarrow$perpendicular reaction pathway of S_1 stilbene (1200 cm^{-1}).[49–53] However, $\gamma_{2\rightarrow p^*}$ at 298 K is estimated to be about $(2\text{ ps})^{-1}$ which is more than ten times larger than the *trans*$\rightarrow$perpendicular reaction rate of S_1 stilbene.[50,52,53] It is of great importance to check whether such an ultrafast process can still be interpreted in terms of the ordinary transition-state formalism that assumes the equilibrium between the reactant and the transition state. The present data are not good enough to bring up a new temperature-dependence expression of $\gamma_{2\rightarrow p^*}$ instead of Eq. (19). At the present stage, it is appropriate to ascribe the temperature dependence of the quantum yield to the existence of an energy barrier.

In Table II, we see the temperature dependence of the S_2 and S_1 lifetimes. Since $\gamma_{2\rightarrow 1}$ is about four times larger than $\gamma_{2\rightarrow p^*}$, the S_2 lifetime depends on T only weakly. The S_2 lifetime change on going from 269 to 298 K is estimated as 0.05 ps by using the relation $\gamma_2=\gamma_{2\rightarrow 1}+a_{2\rightarrow p^*}\exp(-E_a/k_BT)$. The experimental errors of the S_2 lifetime in Table II are too large to know whether the S_2 lifetime depends on T or not. The observed S_1 lifetime change is larger than the experimental errors. The S_1 lifetime becomes longer with decreasing temperature. This temperature dependence of the S_1 lifetime is already well-known. The nonradiative $T_1\rightarrow S_0$ intersystem crossing rate generally decreases with decreasing temperature. On the assumption of $\gamma_1\propto\exp(-E_{S1\rightarrow T}/k_BT)$, the activation energy of the $S_1\rightarrow T_1$ intersystem crossing ($E_{S1\rightarrow T}$) is estimated as 6×10^2 cm^{-1}. It seems that the intersystem crossing from the S_1 state to the T_1 state in all-*trans* retinal is accompanied with a structural change along a coordinate other than that of the double-bond isomerization.

There are two independent ways to obtain temperature-dependent S_1 quantum yield, ϕ_{S1}, from the femtosecond UV data. Using Eq. (16), ϕ_{S1} is directly obtained from A whose temperature dependence is given in Table II. In addition, the relative value of ϕ_{S1} is also obtained from the ratio of the area of the S_1 absorption band [Figs. 6(a) and 7(a)] to that of the S_0 [Figs. 6(b) and 7(b)]. The temperature dependent ϕ_{S1} values obtained by the former method and those by the latter with a proper scaling factor are compared in Fig. 12. They approximately coincide with each other. The coincidence of the independently obtained ϕ_{S1} values strongly supports the present isomerization scheme. Note that ϕ_{S1} in the present scheme is equal to the triplet quantum yield ϕ_T. The obtained ϕ_T or ϕ_{S1} value at 298 K is 0.74 ± 0.04 which is slightly higher than the reported ϕ_T values which ranged from 0.43 to 0.7.[32,33,54–56] All the reported ϕ_T values were obtained by means of the $T_n\leftarrow T_1$ absorption measurements with nano- and microsecond time resolution. In the analysis of the $T_n\leftarrow T_1$ absorption spectrum, it was necessary to assume the molar absorption coefficient of T_1 all-*trans* retinal and the effects of multiple excitation had to be taken into account. The femtosecond UV absorption analysis does not need any assumption, and therefore, the present ϕ_T value is more trustworthy than the previously reported values.

We now consider how the isomerization scheme in Fig. 9 becomes compatible with Kinetics Scheme (II) in which isomerization is not included. An ideal SVD analysis of the femtosecond UV data based on the isomerization scheme in Fig. 9 requires three components, the S_1 all-*trans*, S_0 all-*trans*, and S_0 13-*cis* isomers, but in fact only two SVD components were obtained experimentally. It is already shown by the present SVD analysis of the UV data that the S_1 and S_0 all-*trans* species contribute to the two leading SVD components. It is unlikely that all the contribution of the S_0 13-*cis* isomer to the SVD components was neglected in the present SVD analysis, because the S_0 absorption spectra of the all-

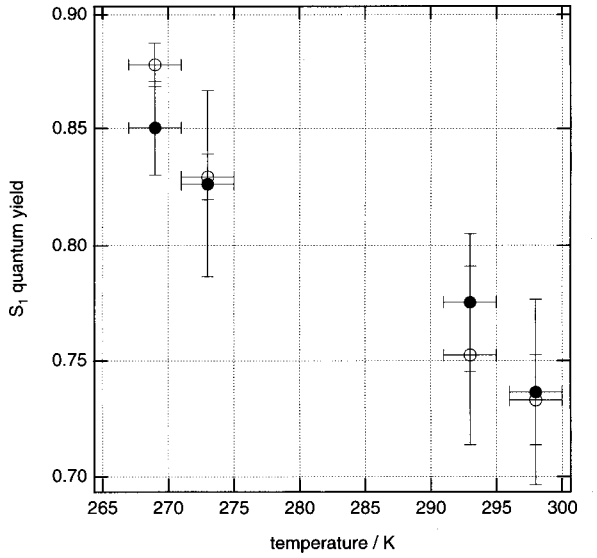

FIG. 12. Temperature dependence of the S_1 quantum yield obtained from the femtosecond UV data by means of two independent methods. One affords absolute values by using isomerization quantum yields (solid circles), and the other gives relative values from absorbance ratio of S_1 to S_0 (open circles).

trans and 13-*cis* isomers are nearly identical. On the contrary, it is highly likely that most of the contribution of the S_0 13-*cis* isomer has already been taken into account in the present SVD analysis, and what was neglected is the contribution of the difference spectrum between the S_0 absorption spectra of the 13-*cis* and all-*trans* isomers. When the temporal evolution of the S_0 all-*trans* isomer is expressed as $f_{S0}(t)$ of Eq. (13), that of the difference spectrum between the 13-*cis* and all-*trans* isomers is written as follows:

$$f_{\mathrm{diff}}(t)=\frac{A}{2}\,(1-e^{-\gamma_p t}). \tag{21}$$

The contribution of each transient species to the SVD components is determined by the product of the area of its absorption spectrum and that of its temporal evolution. The ratio of the area of the S_0 all-*trans* spectrum to that of the 13-*cis*—all-*trans* difference spectrum is obtained from the ground-state absorption spectra as 22.5. The ratio of the area of the S_0 all-*trans* temporal evolution to that of the temporal evolution of the 13-*cis*—all-*trans* difference spectrum is obtained from Eqs. (13) and (21) as 14.5. Accordingly the ratio of the contribution of the S_0 all-*trans* isomer to that of the 13-*cis*—all-*trans* difference spectrum is calculated to be 326. The ratio of the contribution of the S_0 all-*trans* isomer to that of the S_1 all-*trans* isomer is calculated in the same way to be 1.77 from the spectra and the populations in Fig. 6. Consequently the contributions of the S_0 all-*trans* isomer, that of the S_1 all-*trans* isomer, and that of the 13-*cis*—all-*trans* difference spectrum are in the ratio 1:0.57:0.0031. The first through the fourth singular values derived from the femtosecond UV data (Fig. 5) are in the ratio 1:0.44:0.030:0.026, and the third and higher SVD components are dominated by noise. The expected contribution of the 13-*cis*—all-*trans* difference spectrum is ten times smaller than the present noise level. Therefore, the signal to noise ratio has to be improved at least ten times better than in the present experiment, in order to include the contribution of the 13-*cis*–all-*trans* difference spectrum correctly in the SVD analysis with the three components. Owing to both the small difference between the S_0 all-*trans* and 13-*cis* spectra and the low quantum yield of the all-$trans \rightarrow 13\text{-}cis \cdot 9\text{-}cis$ photoisomerization, the SVD analysis of the UV data has been soundly performed with only two components.

No transient absorption band ascribable to p^* was observed either in the VIS region (400–800 nm) or in the near UV region (310–390 nm), though it has been known that the p^* absorption band of tetraphenylethylene is located at 420 nm[48] and that of stiff stilbene is located at 350 nm.[46] It is possible that a p^* absorption band of retinal lies in the wavelength range shorter than 300 nm or longer than 800 nm. It is also noted that the p^* quantum yield of retinal has proved to be as small as 0.26 ± 0.04 in hexane at room temperature, while that of tetraphenylethylene or stiff stilbene is nearly equal to one. Such a small quantum yield makes it difficult to detect the p^* retinal absorption. Since the molar absorption coefficient of p^* is neither known nor predicted, it is not possible to estimate the signal to noise ratio of time-resolved spectra which enables the identification of the p^* absorption by means of the SVD analysis.

Finally, two additional remarks are made on the proposed isomerization scheme in Fig. 9. First, it is possible to ascribe the 7 ps lifetime to the perpendicular ground state, p. A potential minimum at the perpendicular configuration is necessary to account for the lifetime as long as 7 ps. However, existence of such a potential minimum in the ground state has never been rationalized either theoretically or experimentally. The perpendicular ground state whose lifetime is 7.2 ps is much less likely than the perpendicular excited state. Secondly, it is also possible to ascribe the 7 ps lifetime to the vibrationally excited electronic ground state (S_0^*). However, the assignment of p^* to the S_0^* state is not consistent with Fig. 10, which leads to an excellent agreement between the isomerization quantum yields determined by the two independent methods.

V. SUMMARY

The excited-state dynamics and the photoisomerization reactions of all-*trans* retinal in aerated nonpolar solvents were studied by using femtosecond time-resolved UV-VIS absorption spectroscopy. It was found in the time-resolved VIS spectra of all-*trans* retinal that four transient species (S_3, S_2, S_1, T_1) were generated in sequence after the 400 nm photoexcitation. On the assumption that the S_3 state is of $B_u^+(\pi,\pi^*)$ character, the S_2 and S_1 states were characterized as A_g^- (π,π^*) and (n,π^*), respectively. Comparison of the time-resolved VIS spectra of the all-*trans* and 13-*cis* isomers provided no evidence for an isomerization reaction pathway complete within the excited singlet manifold. The femtosecond time-resolved UV absorption spectra of all-*trans* retinal were successfully analyzed in terms of an isomerization scheme involving a perpendicular excited singlet state, p^*. The p^* lifetime was found to be 7.2 ± 2 ps and was much longer than the S_3 and S_2 lifetimes but was shorter

than the S_1 lifetime. It is proposed that the precursor of p^* is the S_2 state. The S_1 state does not take part in the isomerization reaction. The quantum yields of the all-*trans* $\rightarrow$13-*cis*·9-*cis* isomerization in the temperature range 269–298 K obtained from the femtosecond time-resolved UV spectra were in good agreement with the reported values measured by HPLC. The S_1 quantum yields obtained from the femtosecond UV data by way of two independent methods were also in good agreement. These agreements strongly support the proposed isomerization scheme. The height of the energy barrier on the reaction pathway from the S_2 state to p^* was estimated as $(1.2\pm0.6)\times10^3$ cm^{-1}.

[1] H. Hamaguchi, in *Vibrational Spectra and Structure*, edited by J. R. During (Elsevier, Amsterdam, 1987), p. 227.
[2] R. M. Hochstrasser and C. K. Johnson, in *Ultrashort Laser Pulses-Generation and Applications*, edited by W. Kaiser (Springer-Verlag, Berlin, 1993), p. 396.
[3] R. A. Mathies, in *Ultrafast Processes in Chemistry and Photobiology*, edited by M. A. El-Sayed, I. Tanaka, and Y. Molin (Blackwell Science, Oxford, 1995), p. 215.
[4] S. Ganapathy and R. S. H. Liu, Photochem. Photobiol. **56**, 959 (1992).
[5] W. H. Waddell and K. Chihara, J. Am. Chem. Soc. **103**, 7389 (1981).
[6] S. Ganapathy and R. S. H. Liu, J. Am. Chem. Soc. **114**, 3459 (1992).
[7] H. Hamaguchi, H. Okamoto, M. Tasumi, Y. Mukai, and Y. Koyama, Chem. Phys. Lett. **107**, 355 (1984).
[8] Y. Hirata, N. Mataga, Y. Mukai, and Y. Koyama, Chem. Phys. Lett. **134**, 166 (1987).
[9] T. Tahara, B. N. Toleutaev, and H. Hamaguchi, J. Chem. Phys. **100**, 786 (1994).
[10] T. Yuzawa and H. Hamaguchi, J. Mol. Struct. **352–353**, 489 (1995).
[11] T. Takemura, P. K. Das, G. Hug, and R. S. Becker, J. Am. Chem. Soc. **100**, 2626 (1978).
[12] G. Drikos, P. Morys, and H. Rüppel, Photochem. Photobiol. **40**, 133 (1984).
[13] G. Drikos and H. Rüppel, Photochem. Photobiol. **40**, 93 (1984).
[14] G. Drikos, H. Rüppel, W. Sperling, and P. Morys, Photochem. Photobiol. **40**, 85 (1984).
[15] W. H. Waddell, A. M. Schaffer, and R. S. Becker, J. Am. Chem. Soc. **95**, 8223 (1973).
[16] R. R. Birge, J. A. Bennett, B. M. Pierce, and T. M. Thomas, J. Am. Chem. Soc. **100**, 1533 (1978).
[17] R. R. Birge, J. A. Bennett, L. M. Hubbard, H. L. Fang, B. M. Pierce, D. S. Kliger, and G. E. Leroi, J. Am. Chem. Soc. **104**, 2519 (1982).
[18] R. S. Becker, Photochem. Photobiol. **48**, 369 (1988).
[19] S. Alex, H. L. Thanh, and D. Vocelle, Can. J. Chem. **70**, 880 (1992).
[20] J. Papanikolas, G. C. Walker, V. A. Shamamian, R. L. Christensen, and J. C. Baum, J. Am. Chem. Soc. **112**, 1912 (1990).
[21] M. Merchan and R. Gonzalez-Luque, J. Chem. Phys. **106**, 1112 (1997).
[22] R. M. Hochstrasser, D. L. Narva, and A. C. Nelson, Chem. Phys. Lett. **43**, 15 (1976).
[23] A. G. Doukas, M. R. Jnnarkar, D. Chandra, R. R. Alfano, and R. H. Callender, Chem. Phys. Lett. **100**, 420 (1983).
[24] T. Tahara and H. Hamaguchi, Chem. Phys. Lett. **234**, 275 (1995).
[25] S. Yamaguchi and H. Hamaguchi, J. Mol. Struct. **379**, 87 (1996).
[26] E. J. Larson, L. A. Friesen, and C. K. Johnson, Chem. Phys. Lett. **265**, 161 (1997).
[27] S. Takeuchi and T. Tahara, J. Phys. Chem. A **101**, 3052 (1997).
[28] S. Yamaguchi and H. Hamaguchi, Chem. Phys. Lett. **227**, 255 (1994).
[29] S. Yamaguchi and H. Hamaguchi, Appl. Spectrosc. **49**, 1513 (1995).
[30] W. Dawson and E. W. Abrahamson, J. Phys. Chem. **66**, 2542 (1962).
[31] Y. Mukai, Y. Koyama, Y. Hirata, and N. Mataga, J. Phys. Chem. **92**, 4649 (1988).
[32] M. M. Fisher and K. Weiss, Photochem. Photobiol. **20**, 423 (1974).
[33] B. Veyret, S. G. Davis, M. Yoshida, and K. Weiss, J. Am. Chem. Soc. **100**, 3283 (1978).
[34] W. G. Chen and M. S. Braiman, Photochem. Photobiol. **54**, 905 (1991).
[35] T. Iwata and J. Koshoubu, Appl. Spectrosc. **48**, 1453 (1994).
[36] M. Lupu and D. Todor, Chemometrics and Intelligent Laboratory Systems **29**, 11 (1995).
[37] W. H. A. M. Vandenbroek, D. Wienke, W. J. Melssen, C. W. A. Decrom, and L. Buydens, Anal. Chem. **67**, 3753 (1995).
[38] K. Mohanalingam and H. Hamaguchi, Chem. Lett. **1997**, 157.
[39] We note that the inclusion of the direct $S_2 \leftarrow S_0$ photoexcitation in the SVD analysis does not affect the resultant time constants and the quantum yields of the S_1 and T_1 states.
[40] A. Samanta, C. Devadoss, and R. W. Fessenden, J. Phys. Chem. **94**, 7106 (1990).
[41] H. Miyasaka, M. Hagihara, T. Okada, and N. Mataga, Chem. Phys. Lett. **188**, 259 (1992).
[42] M. Ros, M. A. Hogenboom, P. Kok, and E. J. J. Groenen, J. Phys. Chem. **96**, 2975 (1992).
[43] R. J. Sension, S. T. Repinec, A. Z. Szarka, and R. M. Hochstrasser, J. Chem. Phys. **98**, 6291 (1993).
[44] S. Abrash, S. Repinec, and R. M. Hochstrasser, J. Chem. Phys. **93**, 1041 (1990).
[45] J. Saltiel, A. S. Walker, and J. D. F. Sears, J. Am. Chem. Soc. **115**, 2453 (1993).
[46] F. E. Doany, E. J. Heilweil, R. Moore, and R. M. Hochstrasser, J. Chem. Phys. **80**, 201 (1984).
[47] T. Tahara and H. Hamaguchi, Chem. Phys. Lett. **217**, 369 (1994).
[48] B. I. Greene, Chem. Phys. Lett. **79**, 51 (1981).
[49] J. A. Syage, P. M. Felker, and A. H. Zewail, J. Chem. Phys. **81**, 4706 (1984).
[50] H. P. Good, U. P. Wild, E. Haas, E. Fischer, E.-P. Resewitz, and E. Lippert, Ber. Bunsenges. Phys. Chem. **86**, 126 (1982).
[51] J. Saltiel and J. T. D'Agostino, J. Am. Chem. Soc. **94**, 6445 (1972).
[52] M. Sumitani, N. Nakashima, K. Yoshihara, and S. Nagakura, Chem. Phys. Lett. **51**, 183 (1977).
[53] H. Hamaguchi and K. Iwata, Chem. Phys. Lett. **208**, 465 (1993).
[54] R. Bensasson, E. J. Land, and T. G. Truscott, Photochem. Photobiol. **21**, 419 (1975).
[55] R. Bensasson, E. J. Land, and T. G. Truscott, Photochem. Photobiol. **17**, 53 (1973).
[56] T. Rosenfeld, A. Alchalel, and M. Ottolenghi, J. Phys. Chem. **78**, 336 (1974).